Xu *et al. Genome Biology* (2025) 26:137
https://doi.org/10.1186/s13059-025-03605-7

Genome Biology

RESEARCH Open Access

H3K4me3 binding ALFIN-LIKE proteins recruit SWR1 for gene-body deposition of H2A.Z

Linhao Xu[1†], Yafei Wang[2†], Xueying Li[2], Qin Hu[2], Vanda Adamkova[1], Junjie Xu[2], C. Jake Harris[1*] and Israel Ausin[2*]

†Linhao Xu and Yafei Wang contributed equally to this work.

*Correspondence: cjh92@cam.ac.uk; israel.ausin@gmail.com

[1] Department of Plant Sciences, University of Cambridge, Cambridge CB2 3EA, UK
[2] State Key Laboratory for Crop Stress Resistance and High-Efficiency Production, College of Life Sciences and Institute of Future Agriculture, Northwest A&F University, Yangling 712100, Shaanxi, China

Abstract

Background: The H2A.Z histone variant is highly enriched over gene bodies, playing an essential role in several genome-templated processes, including transcriptional regulation and epigenetic patterning across eukaryotes. Deposition of H2A.Z is mediated by the SWR1 remodeling complex. How SWR1 is directed to gene bodies is largely unknown.

Results: Here, we show that ALFIN-LIKE (AL) proteins are responsible for H2A.Z gene body patterning in *Arabidopsis*. AL proteins encode H3K4me3-binding PHD domains, and by ChIP-seq, we confirm preferential binding of AL5 to H3K4me3 over H3K4me1/2 *in planta*. We observe a global reduction in H2A.Z in *al* septuple mutants (*al7m*), especially over H3K4me3-enriched genic regions. While MBD9 recruits SWR1 to nucleosome-free regions, ALs act non-redundantly with MBD9 for deposition of H2A.Z. Notably, *al7m* mutants show severe developmental abnormalities and upregulation of H2A.Z gene body-enriched responsive genes.

Conclusions: Therefore, we propose a model whereby AL proteins direct gene body enrichment of H2A.Z by recruiting SWR1 to H3K4me3-containing responsive genes.

Background

A unique feature of eukaryotic genomes is that their genetic material is organized into chromatin. During chromatin formation, approximately 147 DNA base pairs wrap around a histone octamer consisting of a central H3-H4 tetramer and one H2A-H2B dimer on each side. The resulting structure—known as the nucleosome—serves as the fundamental repeating unit of chromatin [1–3]. While chromatin affords opportunities for genome organization and packaging, nucleosomes represent an inherent obstacle to cellular factors that require access to DNA during processes such as replication, transcription, and DNA repair. Therefore, after initial assembly, chromatin often undergoes dynamic changes in composition, density, and/or post-translational modifications to ensure accessibility and function [4].

One of these dynamic changes in composition involves the exchange of canonical histones by their variants. Histone variants are paralogs that differ from their

canonical partners by a few amino acids or short specific domains [5, 6]. The histone variant H2A.Z is present in all eukaryotic lineages from yeast to metazoans. It has been shown to play crucial roles in several biological processes, such as DNA repair, recombination, or transcription [6, 7]. Interestingly, H2A.Z is associated with both transcriptional stimulation and repression in different genomic contexts, although the molecular mechanisms remain unclear. H2A.Z is generally present at the first nucleosome immediately downstream of the transcriptional start site, i.e., the +1 nucleosome. However, H2A.Z occupancy steeply declines in highly expressed genes in subsequent nucleosomes. In contrast, low-expressed genes are associated with high H2A.Z levels across the gene body [8–10]. H2A.Z can also undergo post-translational modifications that affect transcription. For instance, ubiquitination of H2A.Z can result in repression, while acetylation of H2A.Z may promote activation [8]. Genome-wide, H2A.Z is predominantly located in euchromatic regions and is absent from constitutive heterochromatin [11, 12]. However, it is also present in facultative heterochromatin regions along with H3K4 me3, H3K27 me3, and H2A-Ub [13, 14].

H2A.Z is incorporated into chromatin by the chromatin remodeler SWI/SNF-Related1 complex (SWR1), which replaces H2A-H2B with H2A.Z-H2B dimers [15–17]. Recent studies have used genetic and biochemical approaches to identify the components of the Arabidopsis SWR1. Most of the SWR1 complex components were found to be conserved from yeast, but additional partners were discovered, including METHYL BINDING DOMAIN9 (MBD9), four members of the ALFIN-LIKE family (AL4, 5, 6, and 7), and two subunits of the SAGA complex, TRANSCRIPTION-ASSOCIATED PROTEIN 1 A and 1B [18–20].

How the SWR1 complex is recruited to chromatin remains to be fully resolved. Studies on Arabidopsis and yeast indicate that H3/H4 acetylation may play an important role as the H4 acetyltransferase complex, Nua4, is necessary to maintain H2A.Z patterning, particularly around the +1 nucleosome [21–26]. Furthermore, HISTONE DEACETYLASE 9 (HDA9) and POWERDRESS are required for H2A.Z removal at the *YUCCA8* promoter during thermomorphogenesis [27, 28]. Besides histone acetylation, MBD9 can also direct SWR1 to the promoter of actively transcribed genes [19, 29]

In Arabidopsis, ALs constitute a family of seven members (AL1 to 7) that share high levels of similarity [30–32]. Recombinant AL proteins from Arabidopsis can bind H3K4me2/3 peptides through their PHD domains [30, 32]. *ALFINs* were initially identified as genes involved in *Medicago sativa's* salt-tolerance response [33], and the Arabidopsis ALs have also been implicated in various abiotic stress and physiological processes, such as phosphate starvation, drought, osmotic stress, cold tolerance [34–38], germination, skotomorphogenesis [37, 39], as well as epigenetic silencing [40]. Recently, AL proteins have been identified as interactors with multiple chromatin-related complexes, regulating H3K27me3, histone acetylation, and chromatin accessibility [41]. However, a precise molecular mechanism for the function of AL proteins remains elusive.

Here, we show that the absence of functional AL proteins leads to abnormal development and misregulation of genes bearing the hallmarks of facultative heterochromatin. We show that AL5 interacts with both H3K4me3 and the SWR1 complex in vivo.

Importantly, *al* mutants show a significant reduction in H2A.Z at loci that coincide with AL5 binding. Our findings suggest that ALs recruit the SWR1 complex to chromatin via binding to H3K4me3, facilitating the deposition of H2A.Z at stress-responsive loci.

Results

AL proteins are required for proper development and the control of inducible genes

The seven Arabidopsis ALs are highly related [30–32, 39], and the *al* single mutants do not show any obvious developmental phenotypes under standard growing conditions [38, 39] (Additional file 1: Fig. S1 C). To overcome any potential functional redundancy, we generated higher-order mutants. We obtained *al1-2* to *al3-1* and *al5-1* to *al7-1* from a publicly available seed bank (https://abrc.osu.edu) (Additional file 1: Fig. S1 A and B). However, we could not obtain an *AL4* mutant allele; thus, we generated an *al4-2* allele using CRISPR (Additional file 1: Fig. S1 A and B). The final homozygous AL septuple mutant *al1-2 2–1 3–1 4–2 5–1 6–1 7–1* (hereafter referred to as '*al7m*') shows dramatic developmental defects, including low viability, slow growth, dwarfism, curled leaves, reduced apical dominance, abnormal flowers, and sterility (Fig. 1A, Additional file 1: Fig. S1D), indicating that ALs play a significant role in development.

AL proteins have also been implicated in the response to several abiotic stresses [34–38], suggesting that their role is not restricted to development. To better understand AL function, we performed RNA-seq in the *al7m* and the wild-type control (WT, Col-0). This revealed 1749 genes that are significantly affected by the lack of functional ALs. Among these, approximately three-quarters (1302) are upregulated, while the rest are downregulated (Fig. 1B). Most upregulated genes (960) typically have low expression in WT (Fig. 1C, Additional file 2: Table S1). In contrast, approximately half of the downregulated are low expressed in WT (199), and the remaining sit within the mid (129), high (53), and very high (66) expression categories (Fig. 1D, Additional file 2: Table S1). Gene ontology analysis indicates that upregulated genes are highly enriched for responsive genes (Additional file 1: Fig. S2). Together, these data indicate that the ALs primarily act by repressing transcriptional activity at inducible genes under conditions where their expression is not required.

Next, we investigated key epigenetic features associate with the genes dysregulated in *al7m*. For both up- and down-regulated gene sets, H3K27me3 and H2A.Z levels were higher than the genome average across protein coding genes (PCGs) (Fig. 1E). In contrast, H3K4me3 levels were lower than PCGs in both genesets. Unexpectedly, however, we noticed that the upregulated genes had significantly higher levels of H3K4me3 on average than the downregulated genes, despite the downregulated genes having a much larger proportion of highly expressed genes (see Fig. 1C and D). Similarly, the upregulated geneset is highly enriched for H3K4me2 and the activation-associated H3 acetylation, as compared to both downregulated genes and all PCGs combined. Given that significantly more genes are upregulated than down in *al7m*, and that these up genes are relatively enriched for both repression-associated H3K27me3 and activation-associated marks, the data suggest that AL proteins may specialize in repressing low-expressed or rapidly-turned-over genes with bivalent characteristics (50).

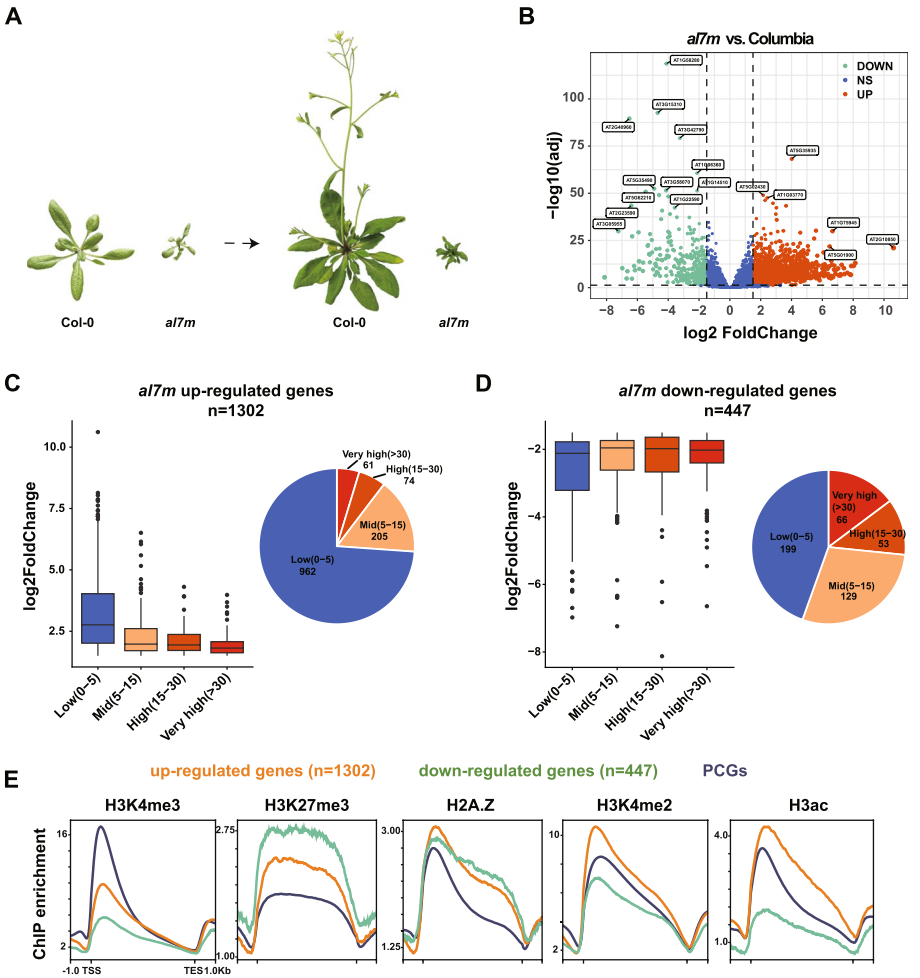

Fig. 1 *alfin-like* septuple mutant (*al7m*) phenotype and analysis of the *al7m* transcriptome. **A** The visual phenotype of the wildtype and *al7m* on 28 (left) and 40 (right) days after germination. **B** Volcano plot showing deregulated genes in the *al7m* mutant background. A cut-off of $\log_2 > \pm 1.5$ and FDR < 0.05 was used for the differential expression level and statistical significance, respectively. **C** Box plot and pie plot showing differential expression of up-regulated genes in *al7m* divided by expression level classes in the wild type. The boxplot's top, mid-line, and bottom represent the upper quartile, median, and lower quartile, respectively. **D** Box plot and pie plot showing differential expression of down-regulated genes in *al7m* divided by expression level classes in the wild type. The boxplot's top, mid-line, and bottom represent the upper quartile, median, and lower quartile, respectively. **E** Metaplots showing the typical profile of the epigenetic marks H3K4me3 (GSE181489), H3K27me3 (SRR10905142), H2A.Z (SRR8695714), H3K4me2 (GSE181489) and H3ac (SRR5837284) over deregulated genes in the *al7m* background and all protein-coding genes (PCGs)

AL proteins bind H3K4me2 and H3K4me3 in planta

The AL proteins have been shown to bind to H3K4me3 in vitro by pull-down with modified histone peptides. AL1,3,4,5 and 7 can also bind to H3K4me2 peptides with lower affinity [30, 32]. To investigate AL binding in vivo, we generated a complementing line (Additional file 1: Fig. S3) expressing AL5 fused to nine copies of the Myc epitope and BLRP. Performing co-immunoprecipitation (Co-IP) analyses, we confirmed that AL5 physically interacts with H3K4me2 and H3K4me3 containing chromatin *in planta* (Fig. 2A). While we cannot exclude the possibility of indirect interactions mediated by adjacent or asymmetric nucleosomes in vivo, these results are consistent with the

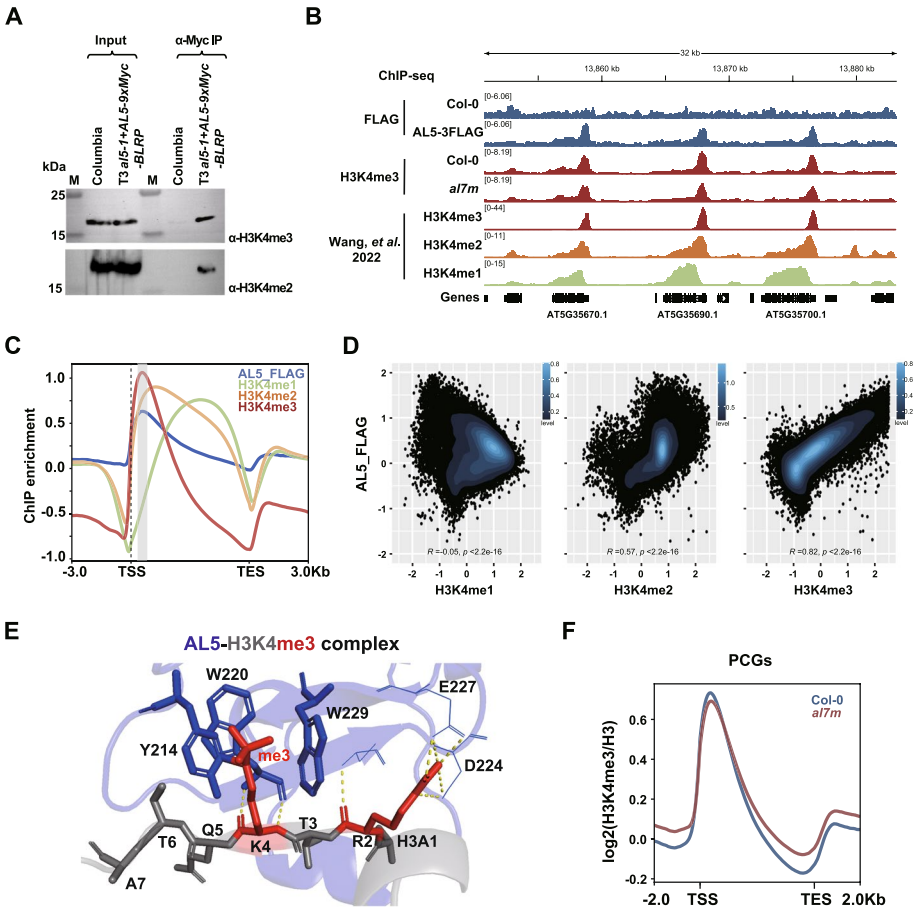

Fig. 2 AL5 is an H3K4me3 binder. **A** Co-immunopurification assays confirming the interaction of AL5 with H3K4me3 and H3K4me2 in *vivo*. Immunoprecipitation lane (α-Myc IP) showing co-purification of AL5. The antibody used to detect the target is indicated at the bottom of the blot. Extracts from the same lines are included to identify the co-precipitating band (Input). **B** Genome browser image showing the colocalization of AL5-FLAG peaks with H3K4me3 peaks at selected genes. **C** Metaplot showing the ChIP-seq signals of AL5-FLAG and published data sets of H3K4me1, H3K4me2 and H3K4me3 (Wang, et al. 2022) over all genes. **D** Scatterplots showing the correlation of AL5-FLAG and H3K4me (Wang, et al. 2022) over all PCGs. Spearman was used as a correlation method. The colored bin represents the density level of dots. **E** AlphaFold three predicted the structure models of the AL5-H3K me3 complex. The AL5 is shown in blue, H3 is shown in grey, and the histone H3K4me3 and H3R2 me peptides are shown in red. AL5 residues involved in H3K4me3 recognition are labeled. **F** Metaplot showing the ChIP-seq signal of H3K4me3 in Col-0 and *al7m* over PCGs

biochemical data and support a model of direct recruitment of ALs to H3K4me3-containing nucleosomes.

Next, we performed ChIP-seq using the *AL5-3xFlag-BLRP* complementing line. (Additional file 1: Fig. S3, S4 A to C). Comparison with available data [42] showed a striking resemblance of the general profile of AL5 to that of H3K4me3 occupancy (Fig. 2B). Metaplot profiles over protein-coding genes showed that AL5 enrichment peaks directly over that of H3K4me3, while H3K4me2 and H3K me1 occupancies peak further downstream in the gene body (Fig. 2C). To quantify the correspondence between AL5 and H3K4me1/2/3, we performed linear regression, revealing a positive correlation with H3K4me2 ($R^2 = 0.57$) and H3K4me3 ($R^2 = 0.82$), and reduced associations with H3K4me1 ($R^2 = -0.05$) (Fig. 2D). We also predicted the structure of the AL5-H3K4me3

complex using AlphaFold3 [43]. The aromatic cage, formed by residues Y214, W220, and W229, along with the H3R2 pocket created by D224 and E227, ensures the binding of AL5 to H3K4me3 (Fig. 2E, Additional file 1: Fig. S5). These results resemble the solved structure of the AL1-H3K4me3 complex [44]. Furthermore, the AL5 signal positively correlates with gene expression states, a well-known characteristic of H3K4me2/3. In contrast, H2A.Z is more abundant in the +1 nucleosome of highly expressed genes and the gene body of lowly expressed genes (Additional file 1: Fig. S4D). We observed that over 96% of the AL5-bound loci ($n = 15{,}336$) overlapped with H3K4me3 peaks (Additional file 1: Fig. S6, Additional file 2: Table S2). These data indicate that AL5 is preferentially recruited to H3K4me3, and to a lesser extent H3K4me2, sites in vivo.

Next, we performed H3K4me3 ChIP-seq in WT versus *al7m* to assess whether ALs are required for H3K4me3 stability (Additional file 1: Fig. S7, Additional file 2: Table S3). We observed minimal perturbation over all genes in aggregate and increased and decreased levels of H3K4me3 at genes that are up-regulated or down-regulated in the *al7m*, respectively (Fig. 2F, Additional file 1: Fig. S8). This correspondence indicates that any changes to H3K4me3 levels in the *al7m* are likely secondary consequences of altered gene expression. To further assess AL's impact on H3K4me3, we focused on AL5 binding sites, finding that fewer than 6% of AL5-bound loci experience loss of H3K4me3 in the *al7m* (876 out of 14,866, Additional file 1: Fig. S7D, S9B). ALs do not appear essential for H3K4me3 maintenance and likely act as genuine 'readers' of H3K4me3 with downstream functions.

AL proteins physically interact with the SWR1 complex in planta

Previous studies have reported a physical interaction between the SWR1 complex and several AL proteins [18–20]. We performed co-immunoprecipitation assays (Co-IP) between AL5 and the SWR1 complex core subunit ARP6, confirming a physical interaction between these components in vivo (Fig. 3A). We also performed immunoprecipitation followed by mass-spectrometry (IP-MS) of AL5-9xMyc-BLRP (Additional file 1: Fig. S3) and identified several components of the SWR1 complex (Additional file 2: Table S4). These data confirm that AL proteins interact with the SWR1 complex *in planta*.

AL proteins are required for the deposition of H2A.Z

As the SWR1 complex is responsible for depositing H2A.Z, we reasoned that ALs might be required for H2A.Z chromatin incorporation. By western blot, we observed an approximate 40% reduction in bulk H2A.Z levels in the *al7m* compared to WT (Fig. 3B, Additional file 1: Fig S10). Next, we conducted ChIP-seq analyses of H2A.Z in WT versus *al7m*. Consistent with the western blot data, this revealed a clear reduction of H2A.Z signal in *al7m* over protein-coding genes. Loss of H2A.Z was most prominent at the 5' end of the transcriptional unit, consistent with the pattern of maximal AL5 enrichment over genes (Fig. 3C to E). Comparing H2A.Z to H3K4me3, we observed a major reduction of H2A.Z, but not H3K4me3, directly over AL5 binding loci (Fig. 4A, Additional file 2: Table S3 and S5) in the *al7m* background. Calling peaks, we found that approximately 41% of AL5 peaks experience coincident loss of H2A.Z in *al7m* (6,095 out of 14,866) (Additional file 1: Fig. S7B and S9 A). We next compared AL5 occupancy to the SWR1 component, PIE1 [20], finding that PIE1 was strongly enriched over AL5-bound

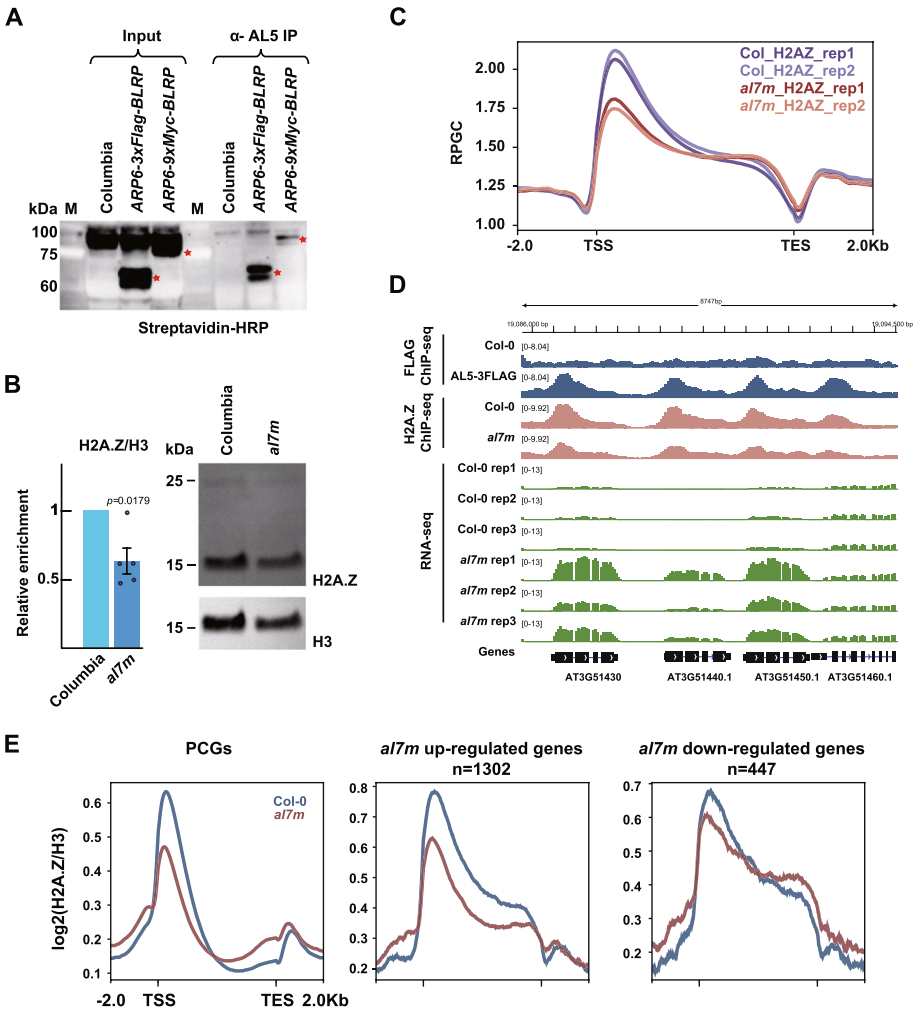

Fig. 3 ALs are required for the deposition of H2A.Z. **A** Co-immunopurification assays confirming the interaction of AL5 with ARP6 in vivo. Immunoprecipitation lane (α-AL5 IP) showing co-purification of AL5. The antibody used to detect the target is indicated at the bottom of the blot. Extracts from the same lines are included to identify the co-precipitating band (Input). The red star indicates ARP6-3xFLAG-BLRP or ARP6-9xMYC-BLRP bands in both input and IP samples. **B** H2A.Z abundance in *al7m*. Western blot (right) and quantification of H2A.Z relative to H3 levels (left) in total histone extracts from the wild type and *al7m*. The upper band in the H2A.Z blot likely represents the ubiquitinated form of H2A.Z. Only the lower band was used for quantification purposes. The data are presented as the average levels of five independent replicates ± SE. A paired two-tailed Student's *t*-test was used to determine the significance between wildtype and *al7m*. **C** Metaplot showing the normalized ChIP-seq signal (RPGC) of H2A.Z in two biological replicates of Col-0 and *al7m* over all PCGs. **D** Genome browser image showing the FLAG ChIP-seq signals of AL5-3 FLAG, H2A.Z ChIP-seq signals of Col-0 and *al7m*, as well as the RNA-seq signals of three biological replicates of Col-0 and *al7m* over representative *al7m* up-regulated genes. **E** Metaplots showing the ChIP-seq signal of H2A.Z in Col-0 and *al7m* over PCGs and *al7m* deregulated genes

regions that lose H2A.Z in the *al7m* (Additional file 1: Fig. S11, Additional file 2: Table S6). To determine whether the loss of H2A.Z is a general effect or is specific to regions bound by AL, we directly compared the loss of H2A.Z over AL5-bound versus unbound loci, finding a significantly stronger reduction over AL5-bound loci (Fig. 4B). Finally, we compared the dynamics of H2A.Z occupancy to the enrichment of AL5 over the transcriptional unit, finding a clear anticorrelation whereby regions most enriched

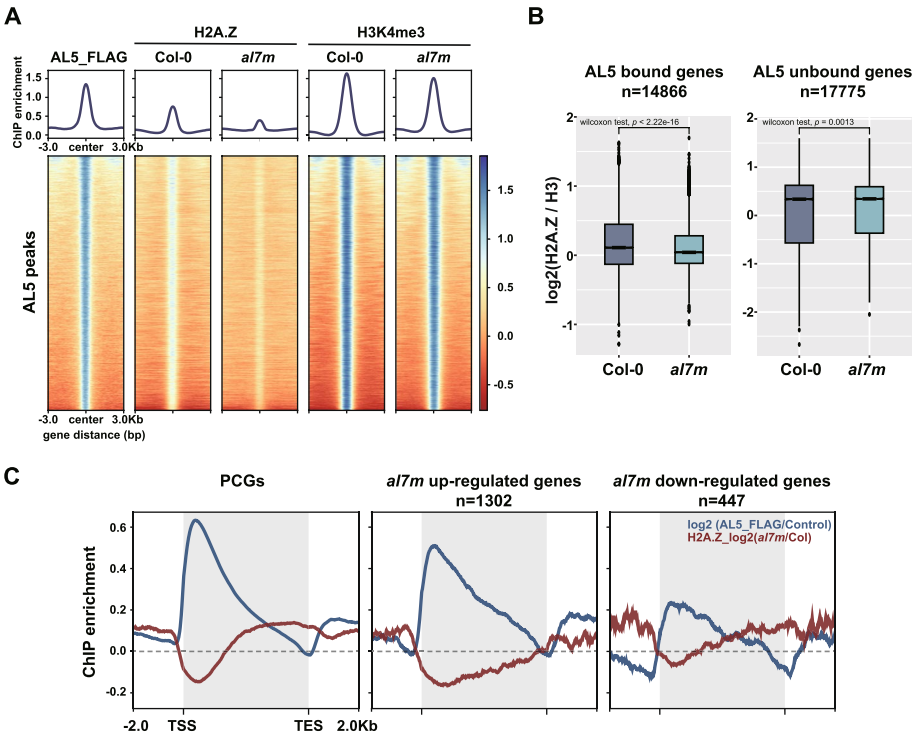

Fig. 4 ALs repress transcription via gene body H2A.Z deposition. A Metaplots and heatmaps showing the ChIP-seq signals of FLAG, H2A.Z, and H3K4me3 over AL5 peaks ($n = 15{,}705$) in Col-0 and *al7m*. **B** Boxplots showing the H2A.Z levels over AL5 bound genes ($n = 14{,}866$) and AL5 unbound genes ($n = 17{,}775$). The boxplot's top, mid-line, and bottom represent the upper quartile, median, and lower quartile, respectively. Wilcoxon test was used to determine the significance. **C** Metaplots showing the ChIP-seq enrichments of AL5-FLAG and H2A.Z over all PCGs and *al7m* deregulated genes

for AL5 experienced the largest losses of H2A.Z in *al7m* (Fig. 4C). Interestingly, the *al7m* upregulated genes experience loss of H2A.Z throughout the gene body. In contrast, downregulated genes more closely resembled the pattern over all protein-coding genes, consistent with the downregulated geneset containing direct and indirect AL5 targets (Fig. 4C).

As our RNA-seq data and previous researchers have implicated ALs in control of stimulus response gene expression, we asked whether these genes were more prone to loss of H2A.Z in the *al7m*. Using a previously defined responsive gene list [45], we compared these to H3K4me3-level matched non-responsive genes, finding that the responsive genes tend lose H2A.Z across the entire gene body (Additional file 1: Fig. S12, Additional file 2: Table S7). Importantly, at non-H3K4me3 enriched genes, we see H2A.Z levels remain virtually unchanged. Overall, these data support a model whereby ALs recruit SWR1 for deposition of H2A.Z over gene bodies of responsive H3K4me3-containing genes.

AL proteins recruit SWR1 independently of MBD9

As we previously identified MBD9 as a key component of SWR1 recruitment and H2A.Z deposition, we were interested in comparing the binding pattern of AL5 to MBD9. Using MBD9 ChIP-seq data [19], we observed that MDB9 peaks directly

upstream of the transcriptional start site (TSS, as previously reported) while AL5 peaks downstream of the TSS (Fig. 5A). To gain a higher resolution perspective on the role of nucleosome positioning, we mapped the AL5 and MBD9 ChIP-seq data over the TSS in comparison to MNase-seq data [46]. As previously reported, maximal MBD9 enrichment corresponded to the nucleosome-free region directly upstream of the TSS. Interestingly, AL5 peaked over the +2 nucleosome downstream of the TSS (Fig. 5B). As both MBD9 and AL5 appear involved in H2A.Z deposition but show some distinct patterns of localization throughout the genome, we asked whether they function redundantly or independently. We identified 7,004 MBD9 and 10,954 AL5 unique peaks and 4,751 common peaks. Over the MBD9 unique peaks, H2A.Z was

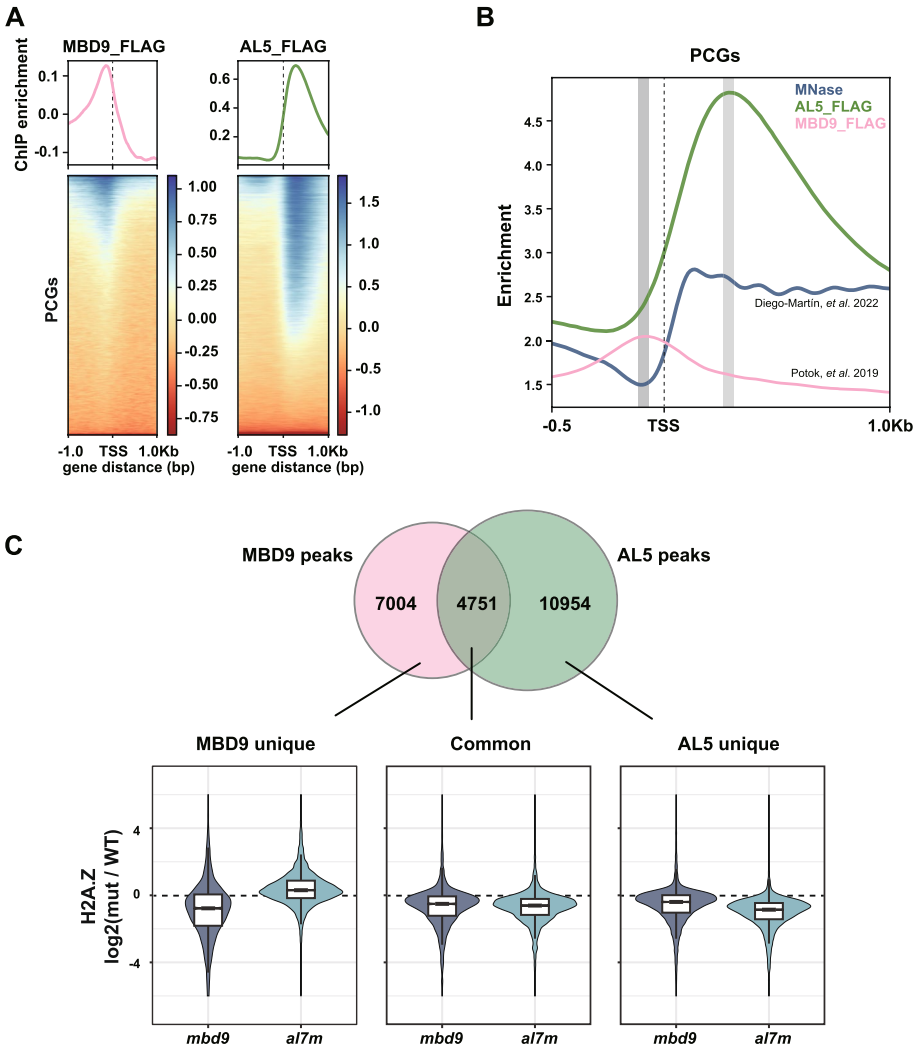

Fig. 5 Comparison between AL5-FLAG and MBD9-FLAG ChIP-seq. **A** Metaplots and heatmaps showing the FLAG ChIP-seq signals of MBD9-FLAG (Potok, et al. 2019) and AL5-FLAG over all PCGs. **B** Metaplot showing the binding position of MBD9-FLAG (Potok, et al. 2019), AL5-FLAG and the position of nucleosomes around TSS from MNase-seq (Diego-Martín, et al. 2022). **C** Venn diagram (top) analysis of MBD9 peaks and AL5 peaks, and violin plot inlaid with boxplot (bottom) showing H2A.Z levels over MBD9 unique peaks ($n = 7{,}004$), common peaks ($n = 4{,}751$) and AL5 unique peaks ($n = 10{,}954$). The boxplot's top, mid-line, and bottom represent the upper quartile, median, and lower quartile, respectively

significantly depleted in *mbd9-3* but not in *al7m*, while we observed the reciprocal at AL5 unique peaks. Importantly, at the common peaks, both *mbd9-3* and *al7m* were required for H2A.Z maintenance (Fig. 5C, Additional file 2: Table S8).

As nucleosome-free regions—where MBD9 is found—are typically associated with highly expressed genes, while in contrast, our RNA-seq data indicates that low-expressed genes are more affected by AL loss, we asked how gene expression level might affect H2A.Z dynamics in these different mutants. We observed that *mbd9-3* mutants exclusively lose H2A.Z at the 5' TSS region, with more significant losses occurring in the highly expressed MBD9-associated genes (Additional file 1: Fig. S13, Additional file 2: Table S9). In *al7m*, we observed that loss of H2A.Z was broadly similar between the lowly and highly expressed AL-associated genes. However, lowly expressed genes consistently show H2A.Z loss across the entire gene body (from TSS to TTS), while highly expressed genes exhibit a more restricted loss, primarily near the TSS region (Additional file 1: Fig. S13, Additional file 2: Table S9). Together, these data support a model whereby ALs are required to maintain H2A.Z over H3K4 me2/3 regions bound by AL5 and that MBD9 and ALs function non-redundantly at partially overlapping genome regions to maintain H2A.Z patterning (Fig. 6).

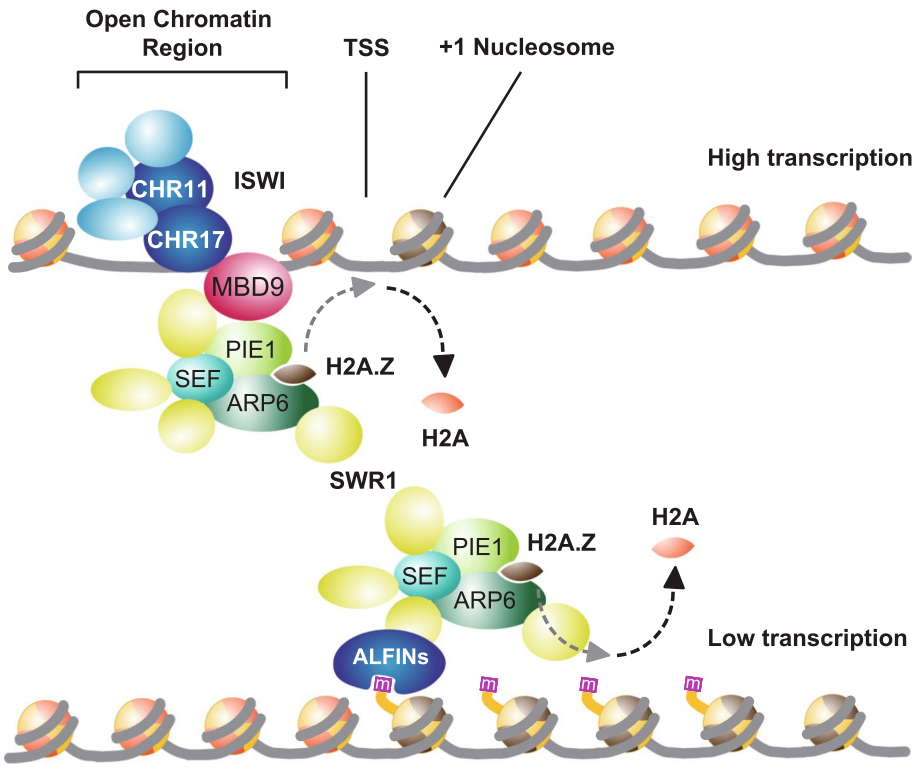

Fig. 6 Proposed model of the role of ALFINs in transcription regulation. Unlike MBD9, which binds to the open chromatin regions and recruits the SWR1 complex to facilitate the deposition of H2A.Z at the + 1 nucleosome, thereby enhancing transcription, ALFINs recognize H3K4me3 marks and recruit the SWR1 complex to deposit H2A.Z within the gene bodies of low-expressed genes

Discussion

The histone variant H2A.Z has been involved in many central aspects of plant biology [7]. However, despite its importance, the precise mechanism by which H2A.Z is selectively deposited in some genomic regions is still unclear. Recently, MBD9 has been reported as a SWR1 interactor [18–20]. MBD9 is likely responsible for recruiting SWR1 to the low-nucleosome regions immediately upstream of the TSS present in highly transcribed genes [19]. This work focused on studying another SWR1 interactor, the AL proteins.

AL proteins have been previously described as H3K4 me3 binding proteins using recombinant proteins and H3-modified peptides [30, 32]. Our research confirms that AL5 tracks H3K4 me3 enriched regions *in planta*, co-localising genome-wide with H3K4me3, and to a lesser extent H3Kme2. While our structural modeling suggests that the PHD domain of AL5 can directly bind H3K4me3, it will be important in future work to confirm this with further biochemical and structural analyses of AL5's histone PTM binding repertoire against that of other plant AL proteins. Notably, we observed that loss of AL has little to no effect on the accumulation of H3K4me3, indicating that ALs do not function in H3K4me3 dynamic regulation but rather act as H3K4me3 readers. In contrast, ALs are required for H2A.Z deposition/maintenance, as we observed a significant decrease in this variant at AL5-bound loci. This is consistent with previous reports of physical interaction between several AL proteins and ARP6, a core component of the SWR1 complex [18–20], and suggests that AL proteins play a role in recruiting the SWR1 complex to a subset of H3K4me3 enriched loci.

We studied the phenotype of plants lacking regular expression of all the ALFIN-LIKE homologs found in Arabidopsis (*al7m*). These plants display severe abnormalities throughout development, indicating a vital role for these proteins under standard growing conditions. Moreover, we discovered that the majority of genes misregulated in the *al7m* typically exhibit little or no expression, and upon loss of ALs, their expression is significantly increased. We have also found that this subset of AL misregulated genes bears a combination of epigenetic features that are unusual for lowly transcribed genes, such as unusually high levels of H3K4me3 and H3Ac—which typically decorate more highly transcribed genes—together with high levels of H3K2 me3 and H2A.Z over the gene body—marks usually accompanying genes with low transcription.

Traditionally, H3K4me3 and H3K27me3 have been considered gene activation or suppression indicators, respectively. These epigenetic marks have been long considered to be mutually exclusive. However, recent studies have revealed that they can appear together in specific genomic regions, resulting in a unique chromatin state [13, 14]. The co-existence of H3K4me3 and H3K27 me3 on the same gene is often called bivalency. Bivalency was first described in ESCs for cases where these two epigenetic marks were often found together in developmental genes. In differentiated cells, this bivalency was later resolved in favor of one of the marks, and only a handful of genes remained bivalent [47–50]. In plants, bivalency is also present in a few developmental genes [51] and is also found in numerous stress-responsive genes [52–58]. However, it is worth noting that evidence for true bivalency, i.e. the co-occurrence of H3K27me3 and H3K4me3 on the same (or adjacent) nucleosomes, requires validation through techniques such as sequential ChIP [50]. Another possibility is that these AL targets are highly expressed

but rapidly turned over in certain cell types, and remain transcriptionally repressed in other by H3K27me3. This low stability could explain the unexpectedly high levels of marks associated with transcription (such as H3K4me3 and H3 acetylation) combined with the very low steady-state levels of mRNA as observed by RNA-seq.

Interestingly, in *arp6* mutants, genes involved in biotic [59] and abiotic [60, 61] stress responses appear constitutively active in the absence of the triggering signal. Moreover, H2A.Z has also been described as a histone variant promoting gene expression responsiveness in Arabidopsis [9]. In contrast, gene body methylation is anti-correlated with gene responsiveness and H2A.Z [45], although whether this is a direct effect or a consequence of low H2A.Z is still unknown. H3K4me3 is also associated with stress responsiveness and transcriptional memory [57, 58, 62, 63]. Thus, it is tempting to speculate that AL proteins are specialized to regulate stress-responsive loci, directing the deposition of H2A.Z to genes poised for rapid activation. In the future, it will be important to determine the nature and positioning of ALs within SWR1 to afford dynamic recruitment of the complex and to understand how the ALs themselves are regulated.

Conclusions

In summary, our study establishes ALFIN-LIKE (AL) proteins as crucial epigenetic regulators in Arabidopsis, playing essential roles in both development and gene expression control. We found that AL proteins, particularly AL5, can preferentially bind to H3K4me3-enriched regions and recruit the SWR1 through physical interaction to facilitate the deposition of H2A.Z over gene bodies. This function is non-redundant with MBD9, which predominantly targets open chromatin regions, primarily upstream of highly expressed genes. Notably, the loss of ALs leads to severe developmental defects and widespread transcriptional misregulation, accompanied by a significant reduction of H2A.Z over gene bodies, particularly at lowly expressed genes. Altogether, our findings reveal a mechanistic link between histone modification recognition, chromatin remodeling, and transcriptional regulation, positioning AL proteins as key modulators of gene expression flexibility in plants.

Methods

Plant material

All the plant materials used in this work are in Columbia (Col-0) background. We obtained *ALs* mutant alleles from ABRC (https://abrc.osu.edu): *al1-2* (Sail_1146_C08), *al2-1* (Sail_663_E04), *al3-1* (SALK_080056), *al5-1* (SALK_075676), *al6-1* (SALK_060877), and *al7-1* (SALK_032503). We generated *al4-2* using CRISPR-Cas9.

Generation of al4-2

The sequence 5'-GAAACACAGTGTGGAGCAATG-3' was used as the PAM cloned into the plasmid pHEE401 [64]. We used the pHEE401 plasmid containing our PAM in Arabidopsis plants. We then selected T_1 transformants using MS plates containing 35 mg/L of hygromycin. We screen the transformants by sequencing around the region targeted by our PAM. We harvested seeds from plants carrying mutations for further analysis in T_2. In the T_2, we selected plants negative for Cas9 and homozygous for the

al4-2 mutation. We backcrossed the original *al4-2* twice against Columbia to minimize possible off-target mutations.

RNA-Seq

We extracted total RNA from 28-day-old plants using TRIzol (Invitrogen). The supernatant containing total RNA was further purified using AxyPrep Multisource Total RNA (Axygen). We sent RNA samples from five biological replicates to BGI genomics (https://www.bgi.com) for sequencing.

The raw reads were first filtered with fastp (version 0.22.0) for low-quality reads, then mapped against the reference genome (TAIR10) using hisat2 (version 5.4.0). The transcriptome was quantified using a subread software, and the GTF file annotated by araport11 was used as the annotation file. We used DEseq2 to analyze differential expression. We used the PCAtools software package to perform PCA analysis and tidyverse to process the data further. We used ggplot2 to draw the volcano plot, boxplot, and pie chart. We used ComplexHeatmap to draw heat maps and classify genes according to expression and correlation coefficient. We used ClusterProfiler for the GO enrichment analysis of differentially expressed genes. we used a q-value cut off = 0.05, and a *p*-value cut off = 0.05. We used org.at.tail.db software package for GO annotation.

Chromatin immunoprecipitation

For the ChIPs of the *al7m*, 0.5 g 40-d-old seedlings were harvested alongside Col-0 control. For the ChIPs of AL5-FLAG, 2.0 g 15-d-old whole plants were harvested from ½ MS plates alongside Col-0 control. ChIPs were performed as previously described [65] https://doi.org/https://doi.org/10.7554/eLife.89353.2. For all ChIPs, two biological replicates were performed. The antibodies used were: anti-FLAG M2 (F1804, Sigma-Aldrich), anti-H3K4me3 (ab8580, Abcam), anti-H2A.Z (AS10718, Agrisera) and anti-H3 (ab1791, Abcam). Libraries were generated with NuGen Ovation Ultra Low System V2 kits following the manufacturer's instructions. The libraries were sequenced for PE150 reads in Illumina NovaSeq 6000.

The reads were aligned to the TAIR10 reference genome using Bowtie2 (version 2.5.3), the duplicated reads were removed by Samtools (version 1.19.2). Deeptools (version 3.5.5) was used to generate the tracks using RPGC for normalization. As there were few differences between the biological replicates in all ChIPs, we merged the biological replicates for downstream analysis. The IGV genome browser was used to visualize the data. MACS2 (version 2.2.9.1) was used for peak calling and differential peaks were identified by DiffBind in R. Peaks were annotated by ChIPseeker in R. Deeptools was used to generate the metaplots and heatmaps.

Data processing

For Supplementary Fig. 4D, genes were divided into 10 groups (g1-g10) based on their expression levels, with each group containing 3,284 genes. In Supplementary Fig. 12, gene sets were defined according to the gene responsiveness list from Aceituno et al. (2008) [45]. H3K4me3-containing genes (n = 15,352) and non-H3K4me3-containing genes (n = 13,601) were first identified using Columbia (Wt)-H3K4me3 data from this study. By combining the H3K4me3-containing genes with the gene responsiveness list,

we identified 2,383 genes as H3K4me3-containing non-responsive genes with a responsiveness score of 0. An equal number of genes were classified as H3K4me3-containing responsive genes, with responsiveness scores ranked from highest to 0. For Supplementary Fig. 13, genes from groups 4 and 5 were combined and labeled as H2A.Z gene-body bearing genes, while genes from groups 6 to 10 were categorized as H2A.Z +1 nucleosome-rich genes, as described in Supplementary Fig. 4D for H2A.Z distribution. To further investigate the roles of MBD9 and AL5 in H2A.Z accumulation, we selected genes bound by MBD9 and AL5 from the +1 nucleosome group and the gene body H2A.Z group. These were categorized into highly expressed genes (n = 6,327) and lowly expressed genes (n = 1,609), respectively. All gene lists and chromosomal regions used to generate the figures can be found in Supplementary Data Table 2.

Co-immunoprecipitation

Jin-Song Zhang and Shou-Yi Chen from the State Key Laboratory of Plant Genomics, Institute of Genetics and Developmental Biology, Chinese Academy of Sciences generously provided the α-AL5 antibody used in the case of AL5-ARP6 interaction testing [38]. We used the Dynabeads antibody coupling kit (Invitrogen) to attach the α-AL5 antibody to magnetic beads. We started by grinding 1 g of floral tissue in liquid nitrogen. Then we added 10 mL of IP buffer (50 mM Tris pH 7.6, 150 mM NaCl, 5 mM MgCl2, 10% glycerol, 0.1% NP-40, 0.5 mM DTT, 1 mM, β-mercaptoethanol, 1 mM PMSF, and 1xProtease Inhibitor cocktail (MCE)). We incubated the mixture on ice for 15 min and then spun it at 4,000 g for 10 min at 4 °C. We then filtered the supernatant through a double Miracloth layer (Millipore). We added the magnetic beads previously coupled to the α-AL5 antibody and incubated them for 1 h at 4 °C with gentle rotation. We washed the beads five times with IP buffer and then released the immunoprecipitate by boiling. Finally, we performed Western blotting and detection using Streptavidin-HRP (1:5,000) (Cell Signaling Technology). To test the interaction between AL5H3K4me2 and H3K4me3, the *AL5-9xMyc-BLRP* was precipitated with Myc beads (MCE). The following steps were identical to AL5-ARP6 procedures. An α-H3K4me3 (1:2,000) (Millipore) and α-H3K4me2 (1:3,000) (Millipore) antibodies were used in WBs to detect their respective presence.

Protein extraction and Western blotting

We conducted an analysis of protein expression using western blots. To detect non-histone proteins, we first ground approximately 100 mg of fresh tissue in liquid nitrogen and added 250μL of protein extraction buffer (50 mM Tris HCl, pH-7.4, 1% β-mercaptoethanol, 12% sucrose, 0.1% Triton X-100, 5 mM PMSF). We shook the mix vigorously and let it sit on ice for 15 min before spinning it at 12,000 g at 4 °C. We then transferred the supernatant to a fresh tube, repeating this step twice. Before loading, we mixed the samples with an appropriate volume of 4 × protein loading buffer (250 mM Tris–HCl pH = 6.8, 400 mM DTT, 8% SDS, 40% glycerol, 0.1% bromophenol blue). We denatured the proteins by boiling them for 15 min. We used the EpiQuik™ total histone extraction kit (EPIGENTEK) to detect histones and followed the manufacturer's instructions. We loaded 10–20μL of proteins into 4–12% for total protein or 12% acrylamide gels for histone extracts (Invitrogen). We transferred

the proteins from the gel to an Immobilon-P membrane (Millipore) at 400 mA for 2 h. The antibody dilution used was as follows: Streptavidin-HRP (1:5,000) (Cell Signaling Technology) or α-H3K4me3 (1:2,000) (Millipore) antibody. According to the manufacturer's recommendations, we detected the HRP signal using the Super Signal West Pico Plus™ Chemiluminescent Substrate kit (Thermo).

Supplementary Information

The online version contains supplementary material available at https://doi.org/10.1186/s13059-025-03605-7.

Additional file 1: Fig. S1. *alfin-like* single mutants' alleles and alfin-like mutants' phenotype. Fig. S2. Gene ontology analysis of *al7m* deregulated genes. Fig. S3. Complementation of the *alfin-like5* mutant. Fig. S4. AL5-FLAG ChIP-seq validation. Fig. S5. AlphaFold3 predicted structure models. Fig. S6. AL5 ChIP-seq signal overlaps with H3K4me and H2A.Z. Fig. S7. H3K4me3 and H2A.Z ChIP-seq validation. Fig. S8. Metaplots showing the ChIP-seq signal of H3K4me3 in Col-0 and *al7m* over *al7m* deregulated genes. Fig. S9. Venn diagram analysis showing the overlap of AL5 bound genes with reduced H2A.Z and H3K4me3 genes in *al7m*. Fig. S10. All 5 biological replicates of H2A.Z abundance western blots. Fig. S11. Overlap of PIE1, AL5 binding and H2A.Z reduction in *al7m*. Fig. S12. H3K4me3 and H2A.Z signals over responsive genes. Fig. S13. H2A.Z signal over highly expressed and lowly expressed genes in *al7m* and *mbd9-3*. Fig. S14. Uncropped images for western blots.

Additional file 2: Table S1. Source data of gene lists used to generate the plots and figures in Fig. 1. Table S2. Source data of chromosomal region information used to generate the plots and figures in Fig. S6. Table S3. Source data of chromosomal region information used to generate the plots and figures in Fig. S7. Table S4. Summary of AL5-9MYC IP Mass spec. Table S5. Source data of AL5-FLAG peaks'annotation used to generate the plots and figures in Fig. 4. Table S6. Source data of chromosomal region information used to generate the plots and figures in Fig. S11. Table S7. Source data of chromosomal region information used to generate the plots and figures in Fig. S12. Table S8. Source data of chromosomal region information used to generate the plots and figures in Fig. 5. Table S9. Source data of chromosomal region information used to generate the plots and figures in Fig. S13

Acknowledgements
We thank Jin-Song Zhang and Shou-Yi Chen for the kind gift of the anti-AL5 antibody and Jiang Dan for her technical assistance.

Peer review information
Wenjing She was the primary editor of this article and managed its editorial process and peer review in collaboration with the rest of the editorial team. The peer-review history is available in the online version of this article.

Authors' contributions
LHX, YFW, XYL, QH, VA, and IA conducted the experiments, LHX and JJX analyzed genomic data, CJH, YFW, and IA designed the experiments, and CJH and IA wrote the manuscript with the participation of all the other authors. All authors read and approved the final manuscript.

Funding
The Ausin lab work was supported by the National Science Foundation of China (NSFC) 32370580, 321703059, and 31801025 grants. The work in the Harris lab was supported by the Royal Society (URF\R1\201016) and a European Research Council (ERC)/UK Research and Innovation (UKRI) grant (EP/X025306/1).

Data availability
Previously published data H3K4me1, H3Kme2, H3K4me3 (GSE181489) [42], H3K27me3 (SRR10905142) [66], H3ac (SRR5837284) [67], MBD9 (GSE123263) [19], PIE1-FLAG (GSE139465) [20] and MNase-seq (GSE205112) [46] were used to generate the plots and figures. All sequencing data generated in this study are accessible at the NCBI Gene Expression Omnibus (GEO) under accession number GSE270861 (ChIP-seq) [68] and GSE270862 (RNA-seq) [69].

Declarations

Ethics approval and consent to participate
Not applicable.

Competing interests
The authors declare no competing interests.

Received: 31 August 2024 Accepted: 6 May 2025
Published online: 21 May 2025

References

1. Luger K, Mader AW, Richmond RK, Sargent DF, Richmond TJ. Crystal structure of the nucleosome core particle at 2.8 A resolution. Nature. 1997;389:251–260.
2. Arents G, Burlingame RW, Wang BC, Love WE, Moudrianakis EN. The nucleosomal core histone octamer at 3.1 A resolution: a tripartite protein assembly and a left-handed superhelix. Proc Natl Acad Sci U S A. 1991;88:10148–10152.
3. Kornberg RD. Chromatin structure: a repeating unit of histones and DNA. Science. 1974;184:868–71.
4. Candela-Ferre J, Diego-Martin B, Perez-Alemany J, Gallego-Bartolome J. Mind the gap: Epigenetic regulation of chromatin accessibility in plants. Plant Physiol. 2024;194:1998–2016.
5. Probst AV. Deposition and eviction of histone variants define functional chromatin states in plants. Curr Opin Plant Biol. 2022;69: 102266.
6. Jiang D, Berger F. Variation is important: Warranting chromatin function and dynamics by histone variants. Curr Opin Plant Biol. 2023;75: 102408.
7. Jarillo JA, Pineiro M. H2A.Z mediates different aspects of chromatin function and modulates flowering responses in Arabidopsis. Plant J. 2015;83:96–109.
8. Gomez-Zambrano A, Merini W, Calonje M. The repressive role of Arabidopsis H2A.Z in transcriptional regulation depends on AtBMI1 activity. Nat Commun. 2019;10:2828.
9. Coleman-Derr D, Zilberman D. Deposition of histone variant H2A.Z within gene bodies regulates responsive genes. PLoS Genet. 2012;8:e1002988.
10. Zilberman D, Coleman-Derr D, Ballinger T, Henikoff S: Histone H2A.Z and DNA methylation are mutually antagonistic chromatin marks. Nature. 2008;456:125–129.
11. Deal RB, Topp CN, McKinney EC, Meagher RB. Repression of flowering in Arabidopsis requires activation of FLOWERING LOCUS C expression by the histone variant H2A.Z. Plant Cell. 2007;19:74–83.
12. Yelagandula R, Stroud H, Holec S, Zhou K, Feng S, Zhong X, Muthurajan UM, Nie X, Kawashima T, Groth M, et al. The histone variant H2A.W defines heterochromatin and promotes chromatin condensation in Arabidopsis. Cell. 2014;158:98–109.
13. Jamge B, Lorkovic ZJ, Axelsson E, Osakabe A, Shukla V, Yelagandula R, Akimcheva S, Kuehn AL, Berger F. Histone variants shape chromatin states in Arabidopsis. Elife. 2023;12:1–26.
14. Sequeira-Mendes J, Araguez I, Peiro R, Mendez-Giraldez R, Zhang X, Jacobsen SE, Bastolla U, Gutierrez C. The Functional Topography of the Arabidopsis Genome Is Organized in a Reduced Number of Linear Motifs of Chromatin States. Plant Cell. 2014;26:2351–66.
15. Mizuguchi G, Shen X, Landry J, Wu WH, Sen S, Wu C. ATP-driven exchange of histone H2AZ variant catalyzed by SWR1 chromatin remodeling complex. Science. 2004;303:343–8.
16. Krogan NJ, Baetz K, Keogh MC, Datta N, Sawa C, Kwok TC, Thompson NJ, Davey MG, Pootoolal J, Hughes TR, et al. Regulation of chromosome stability by the histone H2A variant Htz1, the Swr1 chromatin remodeling complex, and the histone acetyltransferase NuA4. Proc Natl Acad Sci U S A. 2004;101:13513–8.
17. Kobor MS, Venkatasubrahmanyam S, Meneghini MD, Gin JW, Jennings JL, Link AJ, Madhani HD, Rine J. A protein complex containing the conserved Swi2/Snf2-related ATPase Swr1p deposits histone variant H2A.Z into euchromatin. PLoS Biol. 2004;2:E131.
18. Sijacic P, Holder DH, Bajic M, Deal RB. Methyl-CpG-binding domain 9 (MBD9) is required for H2A.Z incorporation into chromatin at a subset of H2A.Z-enriched regions in the Arabidopsis genome. PLoS Genet. 2019;15:e1008326.
19. Potok ME, Wang Y, Xu L, Zhong Z, Liu W, Feng S, Naranbaatar B, Rayatpisheh S, Wang Z, Wohlschlegel JA, et al. Arabidopsis SWR1-associated protein methyl-CpG-binding domain 9 is required for histone H2A.Z deposition. Nat Commun. 2019;10:3352.
20. Luo YX, Hou XM, Zhang CJ, Tan LM, Shao CR, Lin RN, Su YN, Cai XW, Li L, Chen S, He XJ. A plant-specific SWR1 chromatin-remodeling complex couples histone H2A.Z deposition with nucleosome sliding. EMBO J. 2020;39:1-16
21. Raisner RM, Hartley PD, Meneghini MD, Bao MZ, Liu CL, Schreiber SL, Rando OJ, Madhani HD. Histone variant H2A.Z marks the 5′ends of both active and inactive genes in euchromatin. Cell. 2005;123:233–248.
22. Ranjan A, Mizuguchi G, FitzGerald PC, Wei D, Wang F, Huang Y, Luk E, Woodcock CL, Wu C. Nucleosome-free region dominates histone acetylation in targeting SWR1 to promoters for H2A.Z replacement. Cell. 2013;154:1232–1245.
23. Yen K, Vinayachandran V, Pugh BF. SWR-C and INO80 chromatin remodelers recognize nucleosome-free regions near +1 nucleosomes. Cell. 2013;154:1246–56.
24. Altaf M, Auger A, Monnet-Saksouk J, Brodeur J, Piquet S, Cramet M, Bouchard N, Lacoste N, Utley RT, Gaudreau L, Cote J. NuA4-dependent acetylation of nucleosomal histones H4 and H2A directly stimulates incorporation of H2A.Z by the SWR1 complex. J Biol Chem. 2010;285:15966–15977.
25. Babiarz JE, Halley JE, Rine J. Telomeric heterochromatin boundaries require NuA4-dependent acetylation of histone variant H2A.Z in Saccharomyces cerevisiae. Genes Dev. 2006;20:700–710.
26. Durant M, Pugh BF. NuA4-directed chromatin transactions throughout the Saccharomyces cerevisiae genome. Mol Cell Biol. 2007;27:5327–35.
27. van der Woude LC, Perrella G, Snoek BL, van Hoogdalem M, Novak O, van Verk MC, van Kooten HN, Zorn LE, Tonckens R, Dongus JA, et al. HISTONE DEACETYLASE 9 stimulates auxin-dependent thermomorphogenesis in Arabidopsis thaliana by mediating H2A.Z depletion. Proc Natl Acad Sci U S A. 2019;116:25343–25354.
28. Tasset C, Singh Yadav A, Sureshkumar S, Singh R, van der Woude L, Nekrasov M, Tremethick D, van Zanten M, Balasubramanian S. POWERDRESS-mediated histone deacetylation is essential for thermomorphogenesis in Arabidopsis thaliana. PLoS Genet. 2018;14: e1007280.
29. Nie WF, Lei M, Zhang M, Tang K, Huang H, Zhang C, Miki D, Liu P, Yang Y, Wang X, et al. Histone acetylation recruits the SWR1 complex to regulate active DNA demethylation in Arabidopsis. Proc Natl Acad Sci U S A. 2019;116:16641–50.
30. Lee WY, Lee D, Chung WI, Kwon CS. Arabidopsis ING and Alfin1-like protein families localize to the nucleus and bind to H3K4me3/2 via plant homeodomain fingers. Plant J. 2009;58:511–24.
31. Song Y, Gao J, Yang F, Kua CS, Liu J, Cannon CH. Molecular evolutionary analysis of the Alfin-like protein family in Arabidopsis lyrata, Arabidopsis thaliana, and Thellungiella halophila. PLoS ONE. 2013;8: e66838.

32. Liang X, Lei M, Li F, Yang X, Zhou M, Li B, Cao Y, Gong S, Liu K, Liu J, et al. Family-Wide Characterization of Histone Binding Abilities of PHD Domains of AL Proteins in Arabidopsis thaliana. Protein J. 2018;37:531–8.
33. Winicov I. cDNA encoding putative zinc finger motifs from salt-tolerant alfalfa (Medicago sativa L.) cells. Plant Physiol. 1993;102:681–682.
34. Bastola DR, Pethe VV, Winicov I. Alfin1, a novel zinc-finger protein in alfalfa roots that binds to promoter elements in the salt-inducible MsPRP2 gene. Plant Mol Biol. 1998;38:1123–35.
35. Chandrika NNP, Sundaravelpandian K, Yu SM, Schmidt W. ALFIN-LIKE 6 is involved in root hair elongation during phosphate deficiency in Arabidopsis. New Phytol. 2013;198:709–20.
36. Tao JJ, Wei W, Pan WJ, Lu L, Li QT, Ma JB, Zhang WK, Ma B, Chen SY, Zhang JS. An Alfin-like gene from Atriplex hortensis enhances salt and drought tolerance and abscisic acid response in transgenic Arabidopsis. Sci Rep. 2018;8:2707.
37. Velez-Bermudez IC, Schmidt W. Chromatin enrichment for proteomics in plants (ChEP-P) implicates the histone reader ALFIN-LIKE 6 in jasmonate signalling. BMC Genomics. 2021;22:845.
38. Wei W, Zhang YQ, Tao JJ, Chen HW, Li QT, Zhang WK, Ma B, Lin Q, Zhang JS, Chen SY. The Alfin-like homeodomain finger protein AL5 suppresses multiple negative factors to confer abiotic stress tolerance in Arabidopsis. Plant J. 2015;81:871–83.
39. Molitor AM, Bu Z, Yu Y, Shen WH. Arabidopsis AL PHD-PRC1 complexes promote seed germination through H3K4me3-to-H3K27me3 chromatin state switch in repression of seed developmental genes. PLoS Genet. 2014;10: e1004091.
40. Sureshkumar S, Bandaranayake C, Lv J, Dent CI, Bhagat PK, Mukherjee S, Sarwade R, Atri C, York HM, Tamizhselvan P, et al. SUMO protease FUG1, histone reader AL3 and chromodomain protein LHP1 are integral to repeat expansion-induced gene silencing in Arabidopsis thaliana. Nat Plants. 2024;10:749–59.
41. Su XM, Yuan DY, Liu N, Zhang ZC, Yang M, Li L, Chen S, Zhou Y, He XJ. ALFIN-like proteins link histone H3K4me3 to H2A ubiquitination and coordinate diverse chromatin modifications in Arabidopsis. Mol Plant. 2025;18:130–50.
42. Wang Y, Fan Y, Fan D, Zhang Y, Zhou X, Zhang R, Wang Y, Sun Y, Zhang W, He Y, et al. The Arabidopsis DREAM complex antagonizes WDR5A to modulate histone H3K4me2/3 deposition for a subset of genome repression. Proc Natl Acad Sci U S A. 2022;119: e2206075119.
43. Abramson J, Adler J, Dunger J, Evans R, Green T, Pritzel A, Ronneberger O, Willmore L, Ballard AJ, Bambrick J, et al. Accurate structure prediction of biomolecular interactions with AlphaFold 3. Nature. 2024;630:493–500.
44. Zhao S, Zhang B, Yang M, Zhu J, Li H. Systematic Profiling of Histone Readers in Arabidopsis thaliana. Cell Rep. 2018;22:1090–102.
45. Aceituno FF, Moseyko N, Rhee SY, Gutierrez RA. The rules of gene expression in plants: organ identity and gene body methylation are key factors for regulation of gene expression in Arabidopsis thaliana. BMC Genomics. 2008;9:438.
46. Diego-Martin B, Perez-Alemany J, Candela-Ferre J, Corbalan-Acedo A, Pereyra J, Alabadi D, Jami-Alahmadi Y, Wohlschlegel J, Gallego-Bartolome J. The TRIPLE PHD FINGERS proteins are required for SWI/SNF complex-mediated +1 nucleosome positioning and transcription start site determination in Arabidopsis. Nucleic Acids Res. 2022;50:10399–417.
47. Bernstein BE, Mikkelsen TS, Xie X, Kamal M, Huebert DJ, Cuff J, Fry B, Meissner A, Wernig M, Plath K, et al. A bivalent chromatin structure marks key developmental genes in embryonic stem cells. Cell. 2006;125:315–26.
48. Voigt P, Tee WW, Reinberg D. A double take on bivalent promoters. Genes Dev. 2013;27:1318–38.
49. Mikkelsen TS, Ku M, Jaffe DB, Issac B, Lieberman E, Giannoukos G, Alvarez P, Brockman W, Kim TK, Koche RP, et al. Genome-wide maps of chromatin state in pluripotent and lineage-committed cells. Nature. 2007;448:553–60.
50. Liu X, Wang C, Liu W, Li J, Li C, Kou X, Chen J, Zhao Y, Gao H, Wang H, et al. Distinct features of H3K4me3 and H3K27me3 chromatin domains in pre-implantation embryos. Nature. 2016;537:558–62.
51. Faivre L, Schubert D. Facilitating transcriptional transitions: an overview of chromatin bivalency in plants. J Exp Bot. 2023;74:1770–83.
52. Kleinmanns JA, Schatlowski N, Heckmann D, Schubert D. BLISTER Regulates Polycomb-Target Genes, Represses Stress-Regulated Genes and Promotes Stress Responses in Arabidopsis thaliana. Front Plant Sci. 2017;8:1530.
53. Kleinmanns JA, Schubert D. Polycomb and Trithorax group protein-mediated control of stress responses in plants. Biol Chem. 2014;395:1291–300.
54. Yamaguchi N, Ito T. JMJ Histone Demethylases Balance H3K27me3 and H3K4me3 Levels at the HSP21 Locus during Heat Acclimation in Arabidopsis. Biomol. 2021;11:852–65
55. Yamaguchi N, Matsubara S, Yoshimizu K, Seki M, Hamada K, Kamitani M, Kurita Y, Nomura Y, Nagashima K, Inagaki S, et al. H3K27me3 demethylases alter HSP22 and HSP17.6C expression in response to recurring heat in Arabidopsis. Nat Commun. 2021;12:3480.
56. Liu N, Fromm M, Avramova Z. H3K27me3 and H3K4me3 chromatin environment at super-induced dehydration stress memory genes of Arabidopsis thaliana. Mol Plant. 2014;7:502–13.
57. Song ZT, Zhang LL, Han JJ, Zhou M, Liu JX. Histone H3K4 methyltransferases SDG25 and ATX1 maintain heat-stress gene expression during recovery in Arabidopsis. Plant J. 2021;105:1326–38.
58. Ding Y, Avramova Z, Fromm M. The Arabidopsis trithorax-like factor ATX1 functions in dehydration stress responses via ABA-dependent and ABA-independent pathways. Plant J. 2011;66:735–44.
59. March-Diaz R, Garcia-Dominguez M, Lozano-Juste J, Leon J, Florencio FJ, Reyes JC. Histone H2A.Z and homologues of components of the SWR1 complex are required to control immunity in Arabidopsis. Plant J. 2008;53:475–487.
60. Kumar SV, Wigge PA. H2A.Z-Containing Nucleosomes Mediate the Thermosensory Response in Arabidopsis. Cell. 2010;140:136–147.
61. Smith AP, Jain A, Deal RB, Nagarajan VK, Poling MD, Raghothama KG, Meagher RB. Histone H2A.Z regulates the expression of several classes of phosphate starvation response genes but not as a transcriptional activator. Plant Physiol. 2010;152:217–225.
62. Kim JM, To TK, Ishida J, Matsui A, Kimura H, Seki M. Transition of chromatin status during the process of recovery from drought stress in Arabidopsis thaliana. Plant Cell Physiol. 2012;53:847–56.
63. Ding Y, Fromm M, Avramova Z. Multiple exposures to drought "train" transcriptional responses in Arabidopsis. Nat Commun. 2012;3:740.

64. Wang ZP, Xing HL, Dong L, Zhang HY, Han CY, Wang XC, Chen QJ. Egg cell-specific promoter-controlled CRISPR/Cas9 efficiently generates homozygous mutants for multiple target genes in Arabidopsis in a single generation. Genome Biol. 2015;16:144.
65. Harris CJ, Zhong Z, Ichino L, Feng S, Jacobsen SE. H1 restricts euchromatin-associated methylation pathways from heterochromatic encroachment. Elife. 2024;12:1–30.
66. Liu Q, Bischof S, Harris CJ, Zhong Z, Zhan L, Nguyen C, Rashoff A, Barshop WD, Sun F, Feng S, et al. The characterization of Mediator 12 and 13 as conditional positive gene regulators in Arabidopsis. Nat Commun. 2020;11:2798.
67. Jin H, Choi SM, Kang MJ, Yun SH, Kwon DJ, Noh YS, Noh B. Salicylic acid-induced transcriptional reprogramming by the HAC-NPR1-TGA histone acetyltransferase complex in Arabidopsis. Nucleic Acids Res. 2018;46:11712–25.
68. Xu L, Wang Y, Li X, Hu Q, Adamkova V, Xu J, Harris CJ, Ausin I. H3K4me3 binding ALFIN-LIKE proteins recruit SWR1 for gene-body deposition of H2A.Z. H2A.Z ChIP(WT and *al7m*), H3K4me3 ChIP (WT and *al7m*), ALFIN-LIKE5-3xFlag ChIP and Flag ChIP. GSE270861. https://www.ncbi.nlm.nih.gov/geo/query/acc.cgi?acc=GSE270861. 2025
69. Xu L, Wang Y, Li X, Hu Q, Adamkova V, Xu J, Harris CJ, Ausin I. H3K4me3 binding ALFIN-LIKE proteins recruit SWR1 for gene-body deposition of H2A.Z. RNA-seq (WT and *al7m*). GSE270862.https://www.ncbi.nlm.nih.gov/geo/query/acc.cgi?acc=GSE270862. 2025

Publisher's Note